Portugaliae Electrochimica Acta 2016, 34(6), 417-432

DOI: 10.4152/pea.201606417

PORTUGALIAE ELECTROCHIMICA ACTA
ISSN 1647-1571

Electrochemical, Adsorption and Anticorrosion Study on Fluvoxamine and its Blends for X80 Steel Protection in Well Acidizing Fluids

Ekemini Ituen,[a,b,*] Abosede James[c] and Onyewuchi Akaranta[b,c]

[a]*Department of Materials Physics and Chemistry, China University of Petroleum, Qingdao, China*
[b]*African Centre of Excellence for Oilfield Chemicals Research, Institute of Petroleum Studies, University of Port Harcourt, Nigeria*
[c]*Department of Pure and Industrial Chemistry, University of Port Harcourt, Nigeria*

Received September 29, 2016; accepted October 29, 2016

Abstract

Corrosion of steel pipes, tubing, and casings in the oilfield by acidizing fluids is a major cause of materials failure. Corrosion of X80 steel in hydrochloric acid, a typical acidizing solution, was probed using gravimetric and electrochemical techniques. Fluvoxamine (FLU) was used as anticorrosive additive to the acid, and monitored between 30 ^{o}C to 90 ^{o}C. FLU offered efficient protection for the X80 steel by inhibition. The inhibitive effect increased with a higher FLU concentration, but decreased as temperature increased. The highest concentration of FLU ($10x10^{-5}$ M) afforded inhibition efficiency of 93.5% and 80.4% in 1 M and 15% HCl, respectively, at 30 ^{o}C. The efficiency decreased to 88.5% and 73.3%, respectively, at 90 ^{o}C. Inhibition efficiency was improved by blending FLU with glutathione, polyethyleneglycol and potassium iodide. Adsorption and thermodynamic studies reveal that the inhibitor functions, by spontaneous exothermic adsorption on X80 surface, were best described by Langmuir adsorption model. Impedance measurement reveals increase in charge transfer resistance with decrease in double layer capacitance. Polarization studies show that FLU acts as a mixed type inhibitor. Scanned micrographs of X80 surface show a lower pitting in the presence of FLU than in the free acid, demonstrating the effectiveness of FLU as X80 steel corrosion inhibitor.

Keywords*:* acid corrosion, charge transfer resistance, corrosion inhibitor, double layer capacitance, SEM, EIS.

Introduction

Acidizing is an important field technique in oil and gas production, comprising wellbore, matrix and fracture acidizing procedures [1]. In wellbore acidizing, acid is used to wash the wellbore in order to remove scales, corrosion products,

* Corresponding author. E-mail address: ekeminiituen@uniuyo.edu.ng

and some acid soluble debris from drilling, completion, production treating or stimulation [2]. Matrix acidizing involves treating the formation with acid beyond the wellbore [3]. In fracturing, acid is forced under high pressure through the well bore into the reservoir rock formation to chemically react with rocks (calcite, limestone and dolomite) and dissolve them, and to open new flow channels and enlarge existing ones [4, 5]. In the process, cracks are produced in the formation, and acidic solution is introduced into the fracture to etch the flow channels and enlarge pore spaces [4]. Techniques for enhanced oil recovery, removal of scales and drilling mud damage are also associated with the introduction of acids [2].

The most commonly used acid in acidizing procedure is HCl, and at a concentration up to 15% [2]. Formic acid, acetic acid and hydrofluoric acid have also been used, and sometimes as a mixture with sulphuric, phosphoric, nitric, citric, methanesulphonic and chloroacetic acids [2, 5, 6]. Hydrochloric acid is more economical and reacts very fast with the formation, but is highly corrosive. Owing to this corrosive nature of HCl, corrosion inhibitors (CIs) are usually added to protect the surface of steel materials from corrosion and pitting. Many corrosion inhibitors have been reported to be effective in various acid solutions in different concentrations [5, 7-9]. However, it is more desirable that a corrosion inhibitor (CI) be cheap and environmentally and people friendly. It should also be easy to synthesize or processed from inexpensive sustainable sources.

Fluvoxamine is a non-toxic compound which has been used as anti-depressant [10], for treatment of obsessive-compulsive disorder (OCD) [11], and as a potent inhibitor of the metabolism of caffeine in vitro [12]. It is also one of the major compounds that can be obtained from seeds of *Griffonia simplicifolia* [13]. Many electron rich sites found in efficient organic corrosion inhibitors reported in literature [5, 7] are also found in the chemical structure of FLU (Fig. 1).

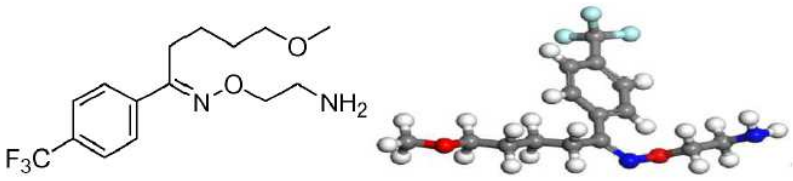

Figure 1. Molecular and ball and stick structures of FLU.

This motivated us to investigate FLU as alternative corrosion inhibitor for acidizing fluid. Different concentrations of HCl were used to simulate acidizing fluids. The X80 steel was used in this study, because such steel grades like API 5L X70, X80, X60, X65, X52 and X42 are extensively preferred for line pipes, transfer tubings, drilling pipes, casings, etc. [14, 15].The use of FLU as corrosion inhibitor for X80 steel is being reported for the first time. Electrochemical and gravimetric techniques were employed to determine the inhibition efficiency and mechanism of inhibition. The morphology of the protected metal is studied using SEM. The effect of temperature on the inhibitor performance is also examined. CI is also blended with synergistic additives to assess their performances at high temperature.

Experimental methods

Preparation of steel specimens

X80 steel specimens with 2 cm x 2 cm dimensions were supplied by Qingdao Tengxiang Instrument and Equipment Co. Ltd., China. As-received surface of X80 steel was treated as provided by NACE Recommended Practice RP-0775 and ASTM G-1 & G-4, for surface finishing and cleaning of weight loss coupons. Coupons for electrochemical studies were abraded with various grades of silicon carbide paper, and 1 cm^2 of the exposed surface was finished to mirror surface with CC-22F P2000 grade of silicon carbide paper. The prepared specimens were enclosed in sealed water-proof bags and stored in moisture free desiccator prior to use. The chemical compositions (wt. %) of X80 were C (0.065), Si (0.24), Mn (1.58), P (0.011), S (0.003), Cu (0.01), Cr (0.022), Nb (0.057), V (0.005), Ti (0.024), B (0.0006), Fe (balance).

Preparation of test solutions

Analytical grade HCl was diluted to concentrations of 1 M and 15% using double-distilled water. As received powdered fluvoxamine (AR), supplied by Meyers Co. Ltd., China, was prepared to different concentrations ($1x10^{-5}$, $3x10^{-5}$, $5x10^{-5}$ and $10x10^{-5}$ M) in HCl solutions. The additives used in blending are: industrial grade polyethyleneglycol, PEG-4000 (PEG) and analytical grade potassium iodide (KI) supplied by Richest group Ltd., Shanghai; analytical grade sodium gluconate (NaG) and industrial grade glutathione (GLU) supplied by Wuhan Yuancheng Gongchuang Technology Co. Ltd., China; and potassium chloride (analytical grade) supplied by Meyer Chemical Technology Co. Lt., Shanghai, China. All reagents were used as supplied, without further analysis or purification. $1x10^{-6}$ M of each additive was blended with $10x10^{-5}$ M FLU in the ratio 1:1 and prepared in the HCl with vigorous stirring.

Weight loss measurement

Weight loss measurements were conducted according to ASTM standard method explained in literature [5]. All weight measurements were conducted using a Sartorius CPA225D analytical balance with sensitivity ±0.00001 g. Pre-weighed X80 coupons were immersed in acid solutions with and without different concentrations of FLU for five (5) hours, and maintained at 30 ^oC in a water bath. The retrieved coupons were cleaned in 20% NaOH solution containing about 200 g/L of zinc dust, dried in air after rinsing in acetone, and weighed to determine the weight loss. This was repeated using the inhibitor blends. Triplicates of the experiments were conducted per test solution, and the means of the weight losses (g) were computed and reported. The corrosion rate (*CR*) of iron, percentage inhibition efficiency (ε_{WL}) and degree of surface coverage (θ) were calculated as follows

$$CR = \frac{87.6\,\Delta W_{mean}}{\rho A t} \qquad (1)$$

$$\varepsilon_{WL} = 100\left(\frac{CR_b - CR_i}{CR_b}\right) \qquad (2)$$

$$\theta = 0.01\varepsilon_{WL} \qquad (3)$$

where ΔW_{mean} is the mean weight loss, CR_b and CR_i are the corrosion rates (cm h^{-1}) in the absence and presence of the inhibitor, ρ is the density of iron (gcm^{-3}), A is the average surface area (cm^2) of the metal specimens, and t is the immersion time (h). The values of corrosion rate obtained were converted to another unit (mmpy) using conversion factors explained in literature [16]. This procedure was repeated at other temperatures such as 45 °C, 60 °C, 75 °C and 90 °C in the different test solutions.

Electrochemical measurements

The electrochemical workstation used for measurement was Gamry ZRA REF 600-18042 Potentiostat/Galvanostat. The conventional three electrode set up was used, consisting of saturated calomel electrode (SCE) as reference electrode, platinum as counter electrode and X80 coupons as working electrode. The EIS were conducted at a frequency of 10 kHz to 10 mHz, for open circuit immersion time of 30 minutes, at 30 °C. The voltage was changed to -0.15 V to +0.15 V vs. E_{OC} at scan rate of 0.2 mV/s for PDP measurements. Linear polarization resistance measurements (LPR) were carried out at -0.20 V to +0.20 V vs. E_{OC} at 1 mV/s. Electrochemical Frequency Modulation (EFM) measurements were conducted using two frequencies: 2 Hz and 5 Hz. The base frequency was 1 Hz, hence, the waveform repeats after 1 s. A peak voltage of 10 mV was used. E-Chem software package was used for data fitting and analysis.

Charge transfer resistance obtained from analysis of Nyquist plot was used to compute the inhibition efficiency according to Eq. 4. The inhibition efficiency from PDP was calculated from the corrosion current densities obtained from analysis of Tafel plot using Eq. 5.

$$\varepsilon_{EIS} = 100\left(\frac{R_{ctI} - R_{ctB}}{R_{ctI}}\right) \qquad (4)$$

where R_{ctB} and R_{ctI} are charge transfer resistances in the absence and presence of the inhibitor, respectively.

$$\varepsilon_{PD} = 100\left(1 - \frac{I_{corr}^{i}}{I_{corr}^{b}}\right) \qquad (5)$$

where I_{corr}^{b} and I_{corr}^{i} are the corrosion current densities in the absence and presence of the inhibitor, respectively. The magnitude of the double layer capacitance (C_{dl}) of the adsorbed film was calculated from constant phase element (CPE), constant (Y_o) and charge transfer resistance (R_{ct}) using Eq. 6.

$$C_{dl} = (Y_0 R_{ct}^{n-1})^{\frac{1}{n}} \qquad (6)$$

where n is a constant showing a degree of roughness of the metal surface obtained from the phase angle, given that $(j^2 = -1)\alpha$ is the phase angle of CPE and $n = 2\alpha/(\pi)$ is the CPE exponent.

SEM study

To study the morphology of the metal in both uninhibited and inhibited solutions, the steel coupons of size 1 cm x 2 cm were abraded to mirror finish, as described above. The SEM images were recorded in the vacuum mode before and after immersion in HCl using AMETEX S4800 SEM/EDAX TSL. This was repeated with a coupon immersed in HCl containing $10x10^{-5}$ M FLU solution. The instrument was operated at 5 kV.

Results and discussion

Weight loss experiment: effect of inhibitor and acid concentration

The corrosion rate (CR), inhibition efficiency (*%I*) and fractional surface coverage obtained from weight loss measurements for the corrosion of X80 in both 1 M HCl and 15% HCl containing the different concentrations of FLU are presented in Table 1.

Table 1. Corrosion rate, inhibition efficiency and fractional surface coverage data for the inhibition of X80 steel corrosion in 1 M and 15% HCl using different concentrations of FLU at 30 ^{o}C.

Concentration	in 1 M HCl			in 15% HCl		
	CR (mmpy)	ε_{WL}(%)	θ	CR (mmpy)	ε_{WL}(%)	Θ
Blank solution	39.45	-	-	69.40	-	-
1 x 10^{-5} M	9.37	76.25	0.76	21.72	68.70	0.69
3 x 10^{-5} M	8.26	79.05	0.79	20.54	70.40	0.70
5 x 10^{-5} M	6.54	83.42	0.83	16.73	75.19	0.75
10 x 10^{-5} M	2.25	94.30	0.94	13.38	80.41	0.80

Inhibition efficiency obtained increased from 76.25% to 94.30%, when the concentration of FLU was increased from $1x10^{-5}$ M to $10x10^{-5}$ M, at constant temperature. The efficiency of FLU was also tested for both 1 M HCl and 15% HCl, and results were compared. The effectiveness of FLU declined when the acid concentration was increased from 1 M to 15%. For instance, the inhibition efficiency decreased from 94.3% in 1 M HCl to 80.4% in 15% HCl at 30 ^{o}C. This represents about a 14.7% decrease in inhibition efficiency on about a 340% increase in acid concentration, which is reasonable and may be improved using some synergistic intensifiers.

Effect of temperature

Nowadays, many industries have ventured into the production and recovery of hydrocarbons from deep pay zones. Since the temperature at the surface is usually different from down-hole temperature, understanding the effect of temperature on a corrosion inhibitor is essential. As one goes down the well, the difference in temperature per unit well length has been described as geothermal gradient. It is believed that the universal average geothermal gradient is about 25 °C per km of depth (1°F per 70 feet of depth) [17, 18]. From literature, the average geothermal gradient in Nigeria Niger delta fields is 28 ^{o}C/km [19].

Therefore, minimally deep wells in the Nigerian Niger-delta region have been reported to be about 2-4 km deep, corresponding to average downhole temperatures of 65-125 ^{o}C [20].
On this basis, the performance of FLU was examined at higher temperatures up to 90 ^{o}C. Results obtained are shown in Table 2. Inhibition efficiency initially increases as temperature increases, and later decreases with higher temperatures. With $10x10^{-5}$ M FLU in 1 M HCl solution, the inhibition efficiency increases from 94.3% at 30 ^{o}C to 95.1% at 60 ^{o}C, before decreasing to 88.5% at 90 ^{o}C. Similar trend was obtained in 15% HCl.

Table 2. Effect of temperature on the inhibition efficiency (%) of $10x10^{-5}$ M FLU as corrosion inhibitor for X80 steel in acidic solutions.

T(^{o}C)	%I in 1 M HCl	%I in 15% HCl
30	94.3	80.4
45	94.7	81.1
60	95.1	83.7
75	92.0	78.0
90	88.5	73.3

This behaviour is graphically illustrated in Fig. 2. This implies that if FLU is used as CI in acidizing fluid, it will perform more efficiently at surface conditions than at down hole conditions. In literature, similar trend of inhibition efficiency is associated with both physical and chemical adsorption mechanism [21].

Effect of additives

It has been reported that certain substances (called intensifiers) can increase the inhibition efficiency of some corrosion inhibitors [5]. Intensifiers are desirable, because corrosion inhibitors often may not provide adequate protection to steels, at high temperatures and long exposure time.

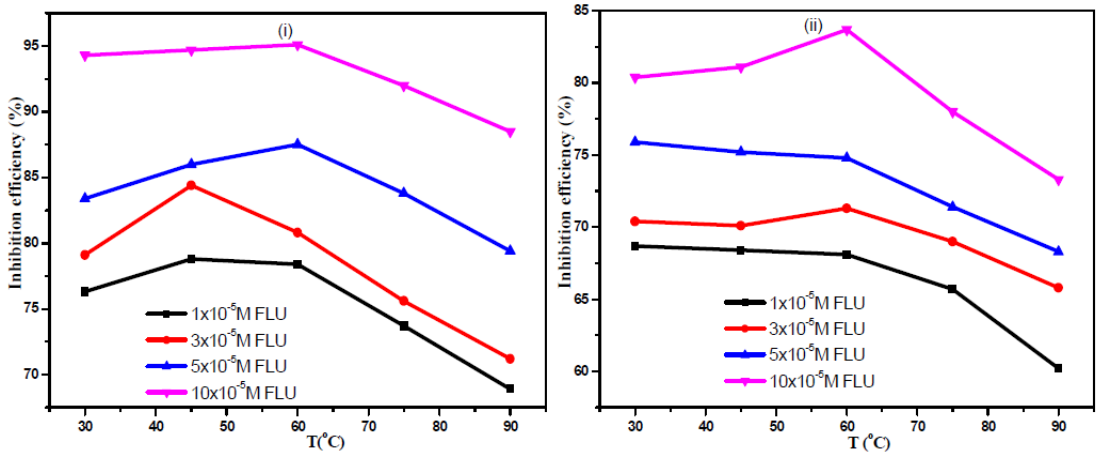

Figure 2. Variation of inhibition efficiency with temperature in (i) 1 M HCl and (ii) 15% HCl.

Therefore, $10x10^{-5}$ M FLU in both 1 M and 15% HCl solutions were blended with potassium iodide (KI), polyethylene glycol (PEG), sodium gluconate (NaG),

and glutathione (GLU). The results obtained (Tables 3-4) show that the additives improved the inhibition efficiency of FLU. For instance, at 90 ºC, the blends containing PEG, KI and GLU afforded *%I* of 93.5%, 94.5% and 95.6 %, respectively, in 1 M HCl and 79.6%, 80.8%, and 84.5% in 15% HCl.

Table 3. Effect of intensifiers on inhibition efficiency (%) of FLU on X80 steel in 1 M HCl solution.

T (ºC)	FLU only	FLU + KI	FLU + PEG	FLU + NaG	FLU + GLU
30	94.3	99.8	99.7	98.9	99.9
45	94.7	98.1	98.9	97.6	99.9
60	95.1	97.5	97.3	96.2	99.8
75	92.0	96.5	96.8	94.8	99.5
90	88.5	93.5	94.5	90.3	98.1

This demonstrates that the inhibitor blends obtained could be suitable alternatives for various oilfield acidizing procedures associated with high temperature operations. However, a study is ongoing to formulate the FLU using surfactants, other intensifiers, solvents, etc., to optimize effectiveness at high temperatures.

Table 4. Effect of intensifiers on inhibition efficiency (%) of FLU on X80 steel in 15% HCl solution.

T(ºC)	FLU only	FLU + KI	FLU +PEG	FLU + NaG	FLU+ GLU
30	80.4	94.6	95.7	88.1	97.5
45	81.1	90.1	91.2	86.2	96.3
60	83.7	85.5	87.6	84.5	94.8
75	78.0	82.7	83.5	79.1	89.6
90	66.3	79.6	80.8	72.4	84.5

Adsorption study

Adsorption of CIs can be either by physical or chemical adsorption mechanism. To predict this mechanism, surface coverage (θ) data were fitted into adsorption models namely, Langmuir, Temkin, Freundlich, Flory Huggins and El-Awady et al. The best fit was obtained with Langmuir isotherm (Fig. 3), with adjusted $R^2 \geq 0.99255$.

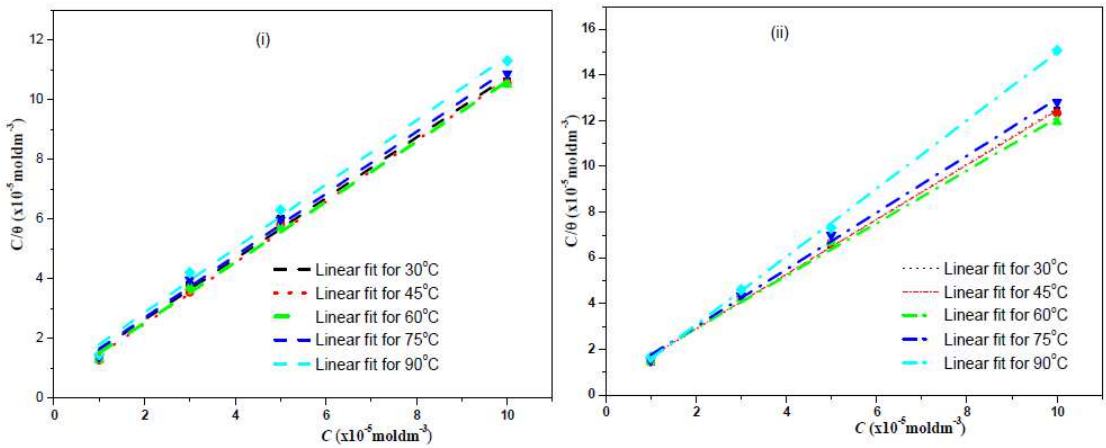

Figure 3. Langmuir adsorption isotherm for the inhibition of X80 steel corrosion in (i) 1 M HCl and (ii) 15% HCl, using different concentrations of FLU.

The expression for the model is given in Eq. 7 [22].

$$\frac{C_{inh}}{\theta} = \frac{1}{K_{ads}} + C_{inh} \qquad (7)$$

where C_{inh} is the concentration of inhibitor (M) in the acid solution and K_{ads} is the adsorption-desorption equilibrium constant, which relates to the free energy change of adsorption (ΔG_{ads}), according to Eq. 8.

$$\Delta G_{ads} = -RT \ln(55.5 K_{ads}) \quad (8)$$

where 55.5 represents the concentration of water molecules displaced by the inhibitor molecules, R is the universal gas constant and T is the absolute temperature. The values of K_{ads} and ΔG_{ads} obtained are given in Table 5.
The constant, $\mathbf{K_{ads}}$, relates to the strength of the inhibitor-metal surface interaction. It can be observed that $\mathbf{K_{ads}}$ decreases as temperature increases, which indicates that the strength of adsorptive binding of FLU to the steel surface decreases as temperature increases, perhaps due to desorption of its molecules from the surface. The $\mathbf{K_{ads}}$ values are also higher in 1 M HCl than in 15% HCl, demonstrating that the inhibitor is more strongly adsorbed on X80 steel in the former than in the later.
The $\mathbf{\Delta G_{ads}}$ values obtained are higher than -40 kJmol$^{-1,}$ suggesting that the mechanism is of chemical adsorption [23]. This indicates that the adsorption of FLU on X80 surface is facilitated by chemical interactions between FLU electrons and empty d-orbitals of iron in the steel. The Langmuir adsorption isotherm assumes equivalent X80 sites with the monolayer of FLU molecules, as shown in the almost unity values of the slope obtained. Therefore, the results obtained are in agreement, since chemisorption mechanism is consistent with monolayer adsorption. In addition, adsorption of FLU is more spontaneous as temperature increases.

Table 5. Parameters deduced from Langmuir adsorption isotherm at different temperatures.

T (°C)	1 M HCl Solution				15% HCl solution			
	K_{ads} (x10^{5}M^{-1})	ΔG_{ads} (kJmol^{-1})	Slope	Adj R^2	K_{ads} (x10^{5}M^{-1})	ΔG_{ads} (kJmol^{-1})	Slope	Adj R^2
30	2.36	-41.28	1.01	0.9925	1.96	-41.67	1.02	0.9979
45	2.37	-43.33	1.03	0.9963	1.99	-42.88	1.11	0.9968
60	2.28	-45.26	1.01	0.9961	1.21	-43.52	1.15	0.9941
75	1.65	-46.38	1.04	0.9942	0.95	-44.78	1.24	0.9966
90	1.41	-47.07	1.07	0.9925	0.63	-46.71	1.39	0.9990

Kinetic and thermodynamic studies

The corrosion rate data were fitted into Arrhenius kinetic model (Eq. 9), and activation energy was calculated from the slope of linear plots of $\log CR$, against reciprocal of temperature (Fig. 4). The obtained activation energy increased on addition of the inhibitor, depending on the inhibitor's concentration. From the concept of activation and collision theory, it can be considered that, before the

acid solution corrodes the steel, the molecules of the acid must collide with the metal molecules on the surface. The acid molecules should possess energy up to a minimum threshold called activation energy.

$$\log CR = \log A - \frac{E_a}{2.303RT} \quad (9)$$

where E_a is the activation energy, A is the Arrhenius pre-exponential factor or frequency factor, R is the universal gas constant and T is the absolute temperature. In the presence of the inhibitors, the activation energy values were higher than in the uninhibited solutions (Table 6). Therefore, the acid molecules must acquire extra (higher) energy in the presence of the inhibitor, for corrosion to occur, hence, corrosion inhibition [24]. The energy also increases as the inhibitor concentration increases. The activation energy was lower in 15% HCl than in 1 M HCl, implying that molecules of 15% HCl solution require a lower energy barrier to cross the activated complex and form corrosion products with mild steel than that of 1 M HCl. The increase in activation energy in the presence of the inhibitor in both acids is consistent with trends reported in literature, and it is associated with physical adsorption mechanism [25].

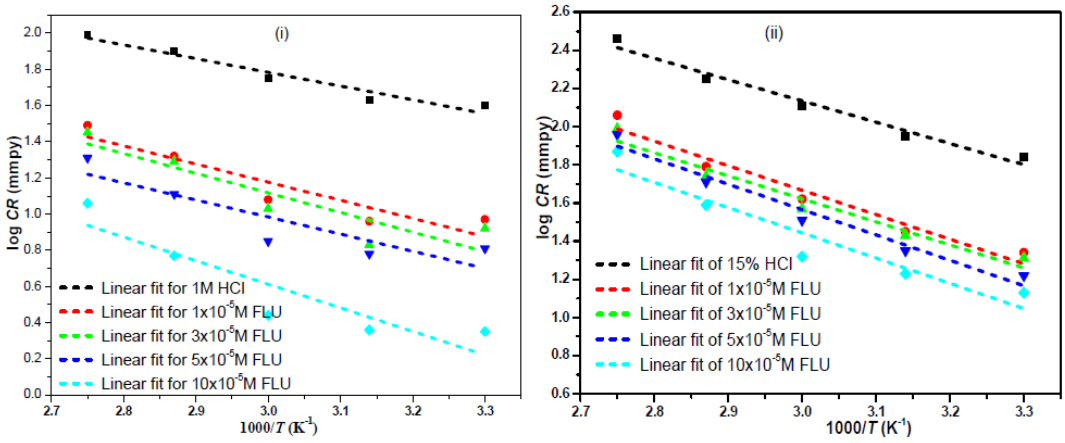

Figure 4. Arrhenius plot for the inhibition of corrosion of X80 steel in (i) 1 M HCl and (ii) 15% HCl, using different concentrations of FLU.

Table 6. Activation and thermodynamic parameters for corrosion of X80 steel in both 1 M HCl and 15% HCl, containing different concentrations of FLU.

FLU Conc ($x10^{-5}$M)	1 M HCl			15% HCl		
	E_a(kJmol^{-1})	ΔH^*(kJmol^{-1})	ΔS^*(kJmol^{-1})	E_a(kJmol^{-1})	ΔH^*(kJmol^{-1})	ΔS^*(kJmol^{-1})
0	14.52	-12.25	0.19	13.01	-14.36	0.12
1	19.16	-24.79	0.17	23.05	-19.55	0.14
3	20.76	-26.35	0.15	24.07	-22.42	0.12
5	26.54	-30.87	0.13	29.53	-26.60	0.10
10	33.87	-33.92	0.11	38.46	-34.09	0.08

The other activation parameters given in Table 6 were derived from the transition state equation (Eq. 10). Linear plots of $\log(\frac{CR}{T})$ against reciprocal of temperature are given in Fig. 5.

$$\log\left(\frac{CR}{T}\right) = \left[\left(\log\left(\frac{R}{Nh}\right) + \left(\frac{\Delta S^*}{2.303R}\right)\right)\right] - \left(\frac{\Delta H^*}{2.303RT}\right) \quad (10)$$

where ΔH^* and ΔS^* are the enthalpy and entropy changes of activation, respectively. The values of ΔS^* are all negative, which implies that a decrease in disorderliness of the system takes place on moving from reactants to the activated complex. It also indicates that the activated complex in the rate determining step involves an association of the inhibitor on metal surface, instead of dissolution of the metal [26]. The negative sign of ΔH^* reflects the exothermic nature of X80 steel corrosion in HCl. Thermodynamically, it is consistent for an exothermic process with decreasing entropy to be spontaneous at temperatures that are not too high [27].

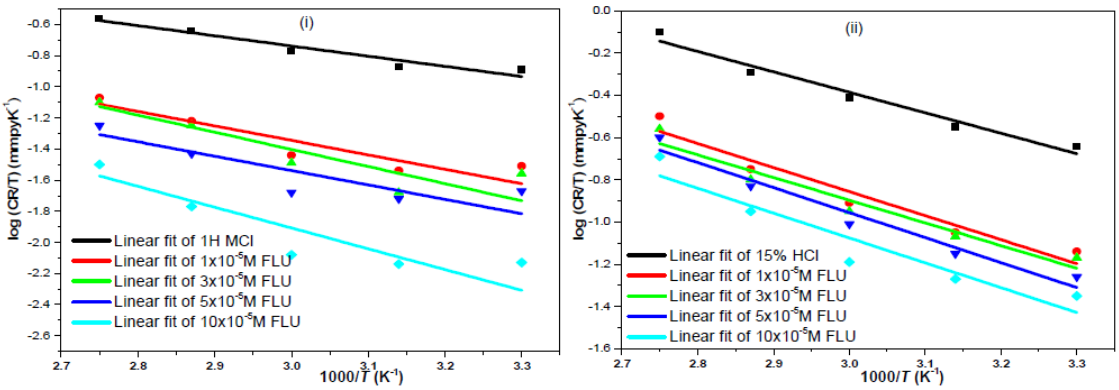

Figure 5. Transition state plots for the corrosion of X80 steel in 1 M and 15% HCl, in the absence and presence of different concentrations of FLU.

EIS experiment

Nyquist and Bode plots shown in Fig. 6 were obtained from analysis of the EIS results for the corrosion of X80 steel in 1 M HCl, with and without different concentrations of FLU. The Nyquist plot yields semicircles with larger diameters in the presence of FLU than in of HCl solution, depending on FLU's concentration.

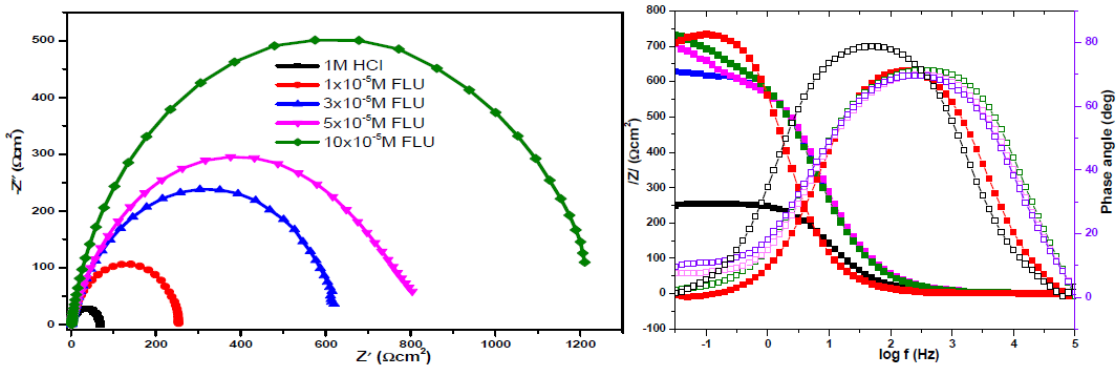

Figure 6. Nyquist (left) and Bode (right) plots for inhibition of X80 steel corrosion in 1 M HCl, using different concentrations of FLU.

The difference in diameter size from that of the HCl solution is due to the influence of FLU on the corrosion rate of X80 steel through the inhibition

process. This is further supported by an increase in diameter, as the inhibitor concentration increases, as it also happens with the obtained inhibition efficiency. The semicircles are imperfect in shape, and this has been attributed to the inhomogeneity of the steel surface, due to adsorption of the inhibitor [28].

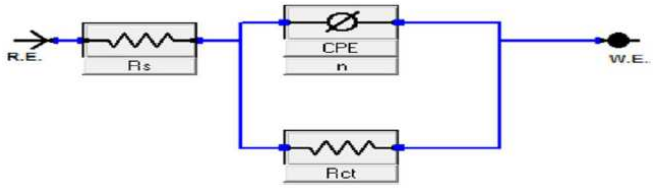

Figure 7. Electrochemical equivalent circuit ($R_s\,(R_{ct}\emptyset_{CPE})$) model used for data fitting.

The shapes of the plots were similar in both the inhibited and free acid solution, indicating that the mechanism of steel corrosion is not influenced by the introduction of FLU. The single capacitive loop obtained also indicates that the mechanism of corrosion is mainly controlled by charge transfer process [26]. The $R_s\,(R_{ct}\emptyset_{CPE})$ equivalent circuit model (Fig. 7) provides a good fit ($\chi^2 \leq 10^{-4}$) for the obtained data.

With this model, a constant phase element (CPE) compensates the surface inhomogeneity of the steel. The CPE is a non-integer element dependent on frequency, and its impedance can be estimated using Y_0 and n in Eq. 11.

$$Z_{CPE} = = (Y_0)^{-1}(jw)^{-n} \qquad (11)$$

where Z_{CPE} is the impedance of the CPE, Y_0 is the CPE constant, w is the angular frequency, j is an imaginary complex number, $(j^2 = -1)\alpha$ is the phase angle of CPE and $n = 2\alpha/(\pi)$.

Some of the EIS parameters calculated are presented in Table 7. The value of n decreases on addition of FLU, indicating that adsorption of FLU molecules increases the surface roughness of the steel [28]. It also shows that there is relative and/or integrated influence on the CPE, rather than just a single resistance, capacitance or inductive element. Decrease in *n* on addition inhibitors also signifies insulation of the metal/solution interface by formation of a surface film. Film formation increases the charge transfer resistance in the presence of the inhibitor. The charge transfer resistance increases with an increase in the inhibitor's concentration, showing that the 'blanketing' property of the film is better at higher inhibitor's concentrations.

Table 7. EIS parameters obtained from Nyquist plots for X80 steel corrosion in 1 M HCl containing different concentrations of FLU.

EIS Parameters	1 M HCl	1x10^{-5} M FLU	3 x 10^{-5} M FLU	5x10^{-5} M FLU	10x10^{-5} M FLU
R_{ct} (Ωcm^2)	30.64	162.4	199.84	239.1	622.9
R_s (Ωcm^2)	1.063	0.963	0.926	0.874	0.790
$Y_o x10^{-6}$ ($\Omega^{-1}s^n cm^{-2}$)	206.4	193.8	190.5	188.2	184.7
n	0.877	0.862	0.847	0.819	0.803
C_{dl} x10^{-9} (F)	12.60	9.03	5.02	4.83	0.16
ε_{wl} (%)	-	81.13	84.47	87.19	95.08

Increase in peak heights of the Bode plots suggests a higher capacitive response of the interface, caused by the presence of the adsorbed inhibitor layer [28], due to the formation of an electrochemical double layer with a magnitude capacitance (C_{dl}) estimated using Eq. 6. The calculated C_{dl} values decrease in the presence of inhibitors, similar to what is reported in literature [28, 29]. This is attributed to a decrease in the local dielectric, or to an increase in the thickness of the double layer or both, caused by the adsorbed protective film of the inhibitors.

PDP experiment

The chemical composition of X80 steel shown above shows that it is a mixture of many metals, hence, a number of oxidation reactions may occur at the anode (Eq. 11). The oxidation of iron in the steel sample is represented by Eq. 13. The reaction at the cathode could involve reduction of water in aqueous environments with sufficiently negative potential (Eq. 14), and/or evolution of hydrogen (Eq. 15).

Anode: $M_{(s)} \rightarrow Mn^{2+}_{(aq)} + ne^-$ (12)

$Fe_{(s)} \rightarrow Fe^{2+}_{(aq)} + 2e^-$ (13)

Cathode: $H_2O + e^- \rightarrow H^+ + OH^-$ (14)

$2H^+_{(aq)} + 2e^- \rightarrow H_{2(g)}$ (15)

The driving force (i.e. potential) was controlled so as to measure the current as a function of the net change in reaction rate. The sum of currents resulting from the electrode processes can be used to obtain the compromise current or free corrosion current density (I_{corr}) and the corresponding potential (E_{corr}) using Tafel plots (Fig. 8).

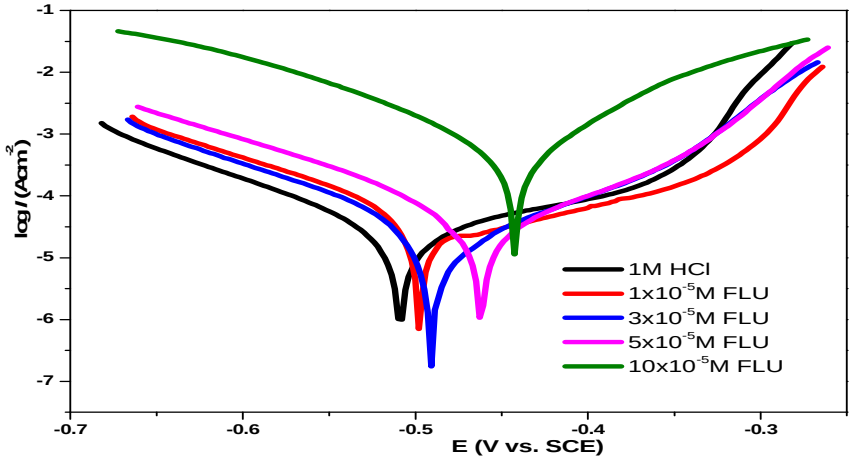

Figure 8. Tafel plots for X80 steel corrosion in 1 M HCl containing different concentrations of FLU.

Also, the cathodic and anodic constants (β_c and β_a) and some other PDP parameters were obtained and are shown in Table 8.

The I_{corr} values decreased with an increase in the inhibitor's concentration, compared to the free acid solution. This is due to the formation of an adsorbed protective film of FLU on the X80's steel surface. A displacement of E_{corr} to

less negative values in the inhibited solutions compared to the free acid solution was also observed. Corrosion inhibitors that displace E_{corr} to less negative values are usually identified as anodic inhibitors, whereas cathodic inhibitors displace the potential to more negative values [30]. Therefore, the E_{corr} values obtained indicate that the inhibitor has dominant influence on the partial anodic reaction. However, the highest difference from that of the free acid (δE_{corr}) is not up to -85 mV, hence, not sufficient to categorize the inhibitor as cathodic or anodic type. Such corrosion inhibitors are usually regarded as mixed type inhibitors with anodic predominance [31]. The obtained values of β_c and β_a differ on addition of inhibitor from those of the free acid solution. The highest difference was obtained with β_a, confirming that FLU exhibits more influence on the anodic reaction.

Table 8. Some PDP parameters for X80 steel corrosion in 1 M HCl, containing different concentrations of FLU.

PDP parameters	1 M HCl	1x10^{-5} M FLU	3x10^{-5} M FLU	5x10^{-5} M FLU	10x10^{-5} M FLU
β_a (mV/decade)	82.1	106.3	107.4	108.2	117.0
β_c (mV/decade)	98.5	99.1	99.8	99.7	103.4
I_{corr} (µA)	693.7	156.5	119.8	102.9	77.5
E_{corr} (mV)	-487.0	-478.8	-473.6	-473.6	-461.0
ε_{PD} (%)	-	77.4	82.7	85.2	88.8

A mixed type inhibitor acts by blocking some active anodic and cathodic sites of the metal, without changing its corrosion mechanism. In other words, FLU inhibits both the iron dissolution and hydrogen evolution processes, but more actively inhibiting iron oxidation (anodic reaction). The mechanism may be activation or diffusion controlled. The calculated inhibition efficiency also increased with an increase in concentration of the inhibitor, similar to EIS results.

LPR measurement

The polarization resistances in the absence and presence of different concentrations of FLU were obtained using insights from the Stern-Geary equation (Eq. 16). Inhibition efficiency was calculated from the polarization resistances using Eq. 17.

$$R_p = \frac{\beta_a \beta_c}{2.303 I_{corr}(\beta_a + \beta_c)} \qquad (16)$$

$$\varepsilon_{RP} = 100\left(\frac{R_{Pi} - R_{Pb}}{R_{Pi}}\right) \qquad (17)$$

where R_{Pi} and R_{Pb} are the polarization resistances with and without the inhibitor, respectively. Obtained values of R_p (Table 9) increased with an increase in FLU's concentration.

The obtained inhibition efficiency followed similar trend as PDP, with respect to concentration. However, the obtained inhibition efficiency was relatively lower than that from PDP measurements, but comparable to EIS results.

Table 9. Some LPR parameters for corrosion of X80 steel in 1 M HCl, containing different concentrations of FLU.

LPR parameters	1 M HCl	1x10^{-5} M FLU	3x10^{-5} M FLU	5x10^{-5} M FLU	10x10^{-5} M FLU
R_p (Ωcm^2)	58.2	219.3	251.7	295.1	403.0
ε_{RP} (%)	-	73.5	76.7	80.3	85.6

EFM measurement

EFM measurement was also carried out using small signals to obtain the causality factors (CF-2 and CF-3) and Tafel constants displayed in Table 10. The obtained causality factors CF-2 and CF-3 are close to theoretical values, indicating that the measurements are of good quality [32]. The slight differences can be attributed to the influence of electrochemical noise on the measurement. Variation in the values of the Tafel constants demonstrates that the inhibitor has more influence on β_a, supporting PDP results.

Table 10. Some EFM parameters for corrosion of X80 steel in 1 M HCl, containing different concentrations of FLU.

Parameters	1 M HCl	1x10^{-5} M FLU	5x10^{-5} M FLU	5x10^{-5} M FLU	10x10^{-5} M FLU
β_a(mV/decade)	83.73	85.13	86.60	87.28	95.34
β_c(mV/decade)	93.44	95.21	97.22	97.08	98.94
CF-2	1.771	1.887	1.823	2.003	2.086
CF-3	2.727	2.897	2.509	2.995	2.553

SEM studies

Micrographs of an abraded X80 steel coupon prior to immersion, and then immersed in 1 M HCl, with and without FLU, for 24 hours, were recorded by SEM. Results reveal that the surface of the coupon immersed in the free acid solution (Fig. 9, left) experienced damage, due to a corrosive attack leading to pitting and undulation. However, the surface of the coupon immersed in the solution containing FLU (Fig 9, right) was relatively smoother compared to the free acid solution.

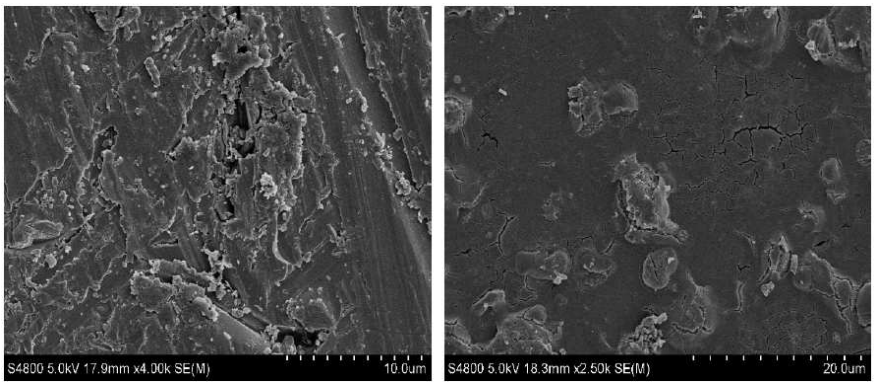

Figure 9. SEM micrographs of abraded X80 steel immersed in 1 M HCl (left) and in 1 M HCl containing 10x10^{-5} M FLU (right).

This demonstrates that the addition of inhibitor reduces the corrosive pitting which occurs in the free acid solution. The extent of protection can be considered to be high, since pitting decreases significantly.
The protective layer formed by the inhibitor was not evenly distributed over the metal surface, which is why some portions on the surface are smoother than others. Thus, the active sites on the steel surface might not be equivalent or possess similar affinity for the active molecules of the inhibitors. Also, some cracks, which may arise during cleaning of the coupon after retrieval, are visible on the protected surface.

Conclusions

Fluvoxamine has been assessed as an alternative anticorrosion additive for X80 steel surface protection in hydrochloric acid. The efficiency of FLU on inhibition of X80 steel corrosion decreases as temperature increases, and increases as FLU concentration increases. Blending of FLU with potassium iodide, polyethyleneglygol and glutathione further improves the efficiency. FLU behaves as a mixed type inhibitor with anodic predominance. Adsorption of FLU on X80 steel surface is spontaneous, exothermic and best described by Langmuir adsorption model. SEM micrographs of X80 steel surface are protected from the aggressive HCl solution by addition of FLU. FLU and its blends could be useful as effective alternative ecofriendly corrosion inhibitors for X80 steel materials in acidic well treatment fluids.

Acknowledgements

The authors acknowledge support from World Bank, through the Robert S. McNamara Fellowship programme, to conduct laboratory work abroad. We also are grateful to Dr. Shuangqing Sun, of Materials Physics and Chemistry Department, China University of Petroleum Qingdao, for providing their facilities and softwares to carry out this research, and to African Centre of Excellence in Oilfield Chemicals Research, for their support. EI is grateful to Prof. A. P. Udoh, Dr. B. S. Antia, Prof. Ogbona Joel, Prof. Hu, Dr. Li, Dr. Wang, Ubong Jerome, Chen, Chao, Xiang and Min in UPC, for their assistance.

References

1. Brezinski MM, Desai B. Google Patents. 1997.
2. Walker ML. Google Patents. 1994.
3. Johannes KF. Gulf Professional Publishing; 2012.
4. Arthur J, Daniel BB, Layne M. Cincinnati: ALL Consulting; 2008.
5. Finšgar M, Jackson J. Corros Sci 2014;86:17.
6. Williams DA, Holifield PK, Looney JR, et al. Google Patents. 1993.
7. Yadav M, Behera D, Sharma U. Arab J Chem. 2012. doi:10.1016/j.arabjc.2012.03.011.
8. Sanyal B. Prog Organic Coat. 1981;9:165.

9. Fouda AS, Shalabi SK, Elewady GY, et al. Int J Electrochem Sci. 2014;9:7038.
10. Burton SW. Int Clin Psychopharmacol. 1991;6:1.
11. Goodman WK, Ward H, Kablinger A, et al. J Clin Psychiat. 1997;58:32.
12. Rasmussen BB, Nielson TL, Brosen K. Pharmacol Toxicol. 1998;83:240.
13. Adotey A. Doctoral Dissertation. 2009.
14. Kennedy JL. Pennwell books, 1993.
15. Masakatsu U, Takabe H, Nice PI. Corrosion. NACE International;2000.
16. Ahmad Z. Butterworth-Heinemann, 2006.
17. Akpabio I, Ejedawe J, Ebeniro J, et al. Global J Pure Appl Sci 2003;9:265.
18. Nwankwo CN, Ekine AS. Int J Phys Sci. 2009;4:777.
19. Adedapo J, Ikpokonte A, Schoeneich K, Kurowska. Gas. 2014;5:12.
20. Emujakporue G, Ekine A. J Earth Sci Geotech Eng. 2014;4:109.
21. Kairi NI, Kassim J. Int J Electrochem Sci. 2013;8:7138.
22. Vinutha MR, Venkatesha TV. Port Electrochim Acta. 2016;34:159.
23. Umoren S, Solomon M. J Ind Eng Chem. 2015;21:81.
24. Nahle, A, Al-Tuniji, RS, Abu-Abdoun, I, Abdel-Rahman, I. Port Electrochim Acta. 2016;34:207.
25. Shukla SK, Ebenso EE. Int J Electrochem Sci. 2011;6:3277.
26. Shaban SM, Aiad I, El-Sukkary, MM, et al. J Mol Liq. 2015;203:20.
27. Patel NS, Hadlicka J, Beranek P, et al. Port Electrochim Acta. 2014;32:395.
28. Anupama KK, Ramya K, Shainy KM, et al. Mater Chem Phys. 2015;167:28.
29. Olasunkanmi LO Mwadham MK, Ebenso EE. Physica E: Low-dimen Sys Nanostruct 2016;76:109.
30. Hamdy A, El-Gendy NS. Egypt J Petrol. 2013;22:17.
31. Alaneme KK, Olusegun SJ, Adelowo OT. Alexan Eng J. 2015;55:673.
32. Fouda AS, Abou Shahba RM, El El-Shenawy A, et al. Elixir Corros Dye. 2015;87:35501.